UCRL-16585

University of California
Ernest O. Lawrence Radiation Laboratory

STRAIN AGING OF IRON ALLOYS

TWO-WEEK LOAN COPY

This is a Library Circulating Copy which may be borrowed for two weeks. For a personal retention copy, call Tech. Info. Division, Ext. 5545

Berkeley, California

DISCLAIMER

This document was prepared as an account of work sponsored by the United States Government. While this document is believed to contain correct information, neither the United States Government nor any agency thereof, nor the Regents of the University of California, nor any of their employees, makes any warranty, express or implied, or assumes any legal responsibility for the accuracy, completeness, or usefulness of any information, apparatus, product, or process disclosed, or represents that its use would not infringe privately owned rights. Reference herein to any specific commercial product, process, or service by its trade name, trademark, manufacturer, or otherwise, does not necessarily constitute or imply its endorsement, recommendation, or favoring by the United States Government or any agency thereof, or the Regents of the University of California. The views and opinions of authors expressed herein do not necessarily state or reflect those of the United States Government or any agency thereof or the Regents of the University of California.

Research and Development

UCRL-16585

UNIVERSITY OF CALIFORNIA

Lawrence Radiation Laboratory
Berkeley, California

AEC Contract W-7405-eng-48

STRAIN AGING OF IRON ALLOYS

Raymond Andrew Busch

(Ph.D. Thesis)

January 1966

CONTENTS

ABSTRACT

I. INTRODUCTION 1

II. PROCEDURE 6

A. Materials and Specimen Preparation 6

B. Apparatus and Testing Technique 7

C. Static Strain Aging Kinetics 8

D. Microscopy 9

III. RESULTS 9

IV. DISCUSSION 13

A. Pure Iron 13

B. Iron-Molybdenum Alloys 14

C. Iron Chromium Molybdenum Alloys 17

D. Strengthening Mechanisms in Static Strain Aging 18

E. Dynamic Strain Aging 20

V. SUMMARY AND CONCLUSIONS 29

Acknowledgements 31

Bibliography 32

Tables 34

Figure Captions 35

Figures 37

STRAIN AGING OF IRON ALLOYS

Raymond Andrew Busch

Inorganic Materials Research Division, Lawrence Radiation Laboratory,
Department of Mineral Technology, College of Engineering,
University of California, Berkeley, California

ABSTRACT

January 1966

The strain aging of iron molybdenum and iron chromium molybdenum alloys has been investigated. Large strengthening effects are observed in both alloys during strain in the 400-500°C range, and in the room temperature properties after this strain. The variation of these effects with impurity content in the iron molybdenum alloy indicates that interstitial solutes are not responsible for the strengthening. The aging of specimens strained at room temperature obeys an activation energy of 42 kcal/mole and $t^{2/3}$ kinetics.

This behavior is interpreted according to the Cottrell-Bilby model for strain aging. The data indicate that a similar process occurs during strain at higher temperatures, which requires the existence of strain enhanced diffusion. The magnitude of this enhancement is estimated as ~100, i.e. the diffusivity during deformation under these conditions is about 100 times greater than the normal diffusivity at the same temperature.

I. INTRODUCTION

When certain alloys are plastically strained and aged at a sufficiently high temperature, they exhibit changes in physical properties which do not occur after either straining or aging alone. The combined process is referred to as "strain aging". Except in a few simplified cases, the mechanism responsible for the property changes is unknown. The phenomenon is of fundamental interest since it involves the fine-scale interactions between solute atoms and dislocations; it is also technologically important due to the property changes, as will be seen below.

The strain aging of steel has been the subject of numerous investigations during the last twenty-five years. Much of this work has been done with mild steel (iron containing about 0.05% carbon) where the main effect of strain aging is the reintroduction of the sharp yield drop and the associated non-uniform deformation. Since these characteristics impair forming operations, attention has been directed toward inhibition of the process. An extensive review of this work has been published by Baird.[1]

More recently it has been found that in higher carbon and alloy steels, strain aging raises the entire stress-strain curve. This has led to investigation of strain aging as a strengthening mechanism, particularly in martensitic alloy steels, but also in ferritic steels intended for elevated temperature service. In the latter connection it should be pointed out that classically, strain aging has referred to straining (usually at room temperature) followed by aging at some higher temperature. Strengthening is also obtained if strain is introduced at an elevated temperature, so that straining and aging occur

simultaneously. The former process is referred to as "static strain aging", the latter as "dynamic strain aging." Three investigations reported in the literature serve to illustrate the difference in properties obtained by the two processes.

Stephenson and Cohen[2] studied the static strain aging of AISI 4340, which is essentially a chromium-molybdenum steel, in the quenched and tempered condition. Specimens were strained in tension, aged at various temperatures, and then tested at room temperature. Large (~ 40,000 psi) increases in yield strength and decreases in ductility (as measured by percent elongation) were observed. Except for specimens which were aged at temperatures high enough to remove the strengthening effect, the strain-aged material exhibited mechanical instability - i.e. necking began at the yield point and subsequent deformation occurred under a falling stress. The authors pointed out that this circumstance made it impractical to utilize the strength increases obtained.

Goel, Busch and Zackay[3] studied the static and dynamic strain aging of H-11, a chromium-molybdenum-vanadium steel similar in carbon content to AISI 4340. Static strain aging produced results similar to those found by Stephenson and Cohen. Dynamic strain aging, followed by a 900°F aging treatment, resulted in similar strength increases while maintaining stable deformation and most of the original ductility, except for specimens strained in the "blue brittle" range of 400-600°F. The latter specimens exhibited mechanical instability.

Peterson[4] studied nominally plain carbon ferritic-pearlitic steels in the 0.1 to 0.8% carbon range (the steels also contained significant amounts of manganese and nitrogen). Strain was introduced by drawing at various temperatures. He found that:

1. Dynamic strain aging produced greater strengthening with smaller loss in ductility than static strain aging;

2. The strengthening produced by dynamic strain aging was independent of carbon content over the entire range studied, while that produced by static strain aging was directly proportional to the carbon content. The dynamic strengthening was related to the nitrogen content.

These experiments suggest that the two types of strain aging involve qualitatively different strengthening mechanisms. In particular, the nitrogen dependence of the dynamic strengthening in Peterson's alloys, which contained appreciable manganese, suggests that substitutional solutes may have an important influence under dynamic conditions. Manganese interacts strongly with nitrogen, as has been shown by internal friction studies,[5] but is not a strong carbide former. Thus the observed dependence of nitrogen may be due to a manganese-nitrogen effect.

Glen[6] has proposed, on the basis of tensile properties of steels containing carbide forming elements, that carbide precipitation during elevated temperature testing is responsible for the observed strengthening effects.

Baird[1] has proposed a mechanism involving the binding of substitutional atoms to carbon or nitrogen atmospheres formed around moving dislocations. Ardley and Cottrell[7] have proposed the direct formation of substitutional atmospheres on the basis of experiments with α brass, and Cottrell[8] has attempted to explain the Portevin-Le Chatelier effect in aluminum alloys on the same model.

Since the normal bulk diffusivity of substitutional atoms at the straining temperatures concerned is too slow for the solute to either diffuse with moving dislovations or move over sufficient distances for

precipitation effects to become important during strain, the mechanisms mentioned above all require the existence of a strain enhanced diffusion effect.

Two theoretical treatments of strain enhanced diffusion have been published. Both apply to the high temperature, low strain rate region (e.g. creep testing); no treatment for the lower temperature, high strain rate region has been published. Baluffi and Ruoff[9] have considered the possibility of enhanced diffusion due to non-equilibrium vacancy concentrations and have concluded that no appreciable diffusion enhancement should occur. Romashkin[10] considered the same mechanism and predicted enhancements of several orders of magnitude under favorable conditions.

The experimental evidence for strain enhanced diffusion is also controversial. For example, Hirano et al.[11] found enhancements of up to a factor of 3000 in iron, Lee and Maddin[12] and Forestieri and Girifalco[13] reported enhancements of about 100 in silver and Wazzan et al.[14] reported an enhancement of 30 in nickel. On the other hand, Darby et al.[15] found no significant enhancement in silver, and similar results have been obtained by Chollet et al.[16] in iron-nickel, Pearson et al.[17] in aluminum-zinc, and Savitskii[18] in iron. The techniques used in most of these experiments have involved direct determination of the diffusivity of solute or tracer atoms, and thus are limited to higher temperatures and lower strain rates than those of interest in strain aging. The studies which have involved the effect of strain on tempering reactions have also been conducted under the former conditions, and are also in conflict with each other.[19,20] The enhancement, when observed, increased with increasing strain rate and decreasing temperature, which suggests that the effect may be important under dynamic strain aging conditions.

At still lower temperatures, the normal diffusivity is so small that segregation effects would not be important even in the presence of a large diffusion enhancement.

The importance of substitutional solute diffusion arises from two factors. First, it is the rate controlling process in the growth of carbide or nitride precipitates, since it is many orders of magnitude smaller than interstitial diffusion. Second, it may control the nucleation of precipitates. Honeycombe[21] reported finding clusters of molybdenum and vanadium in alloy steels prior to the detection of carbides.* Thus, enhanced substitutional solute diffusion may increase both the nucleation and growth rates in tempering reactions.

The present work was concerned with the behavior of substitutional solutes in iron during strain over a range of temperatures. The primary goals were to learn whether these solutes produced strain aging effects in the absence of interstitial impurities; and to relate such effects to the question of strain enhanced diffusion. The findings would then be applied to the strengthening observed in dynamically strain aged alloy steels.

---

* Recent private communication indicates that later results have raised doubts about this finding.

II. PROCEDURE

A. Materials and Specimen Preparation

The alloys studied were prepared from high purity iron, chromium, and molybdenum. The processing and analyses of these materials are indicated in Table I. Alloys were melted in a cold hearth system similar to that described by Berghezan and Simonsen.[22] An iron rod was held horizontally above a water cooled copper hearth. The rod was grooved so that it could be used as a container for the alloying elements which were added as small fragments. All materials were etched, rinsed with distilled water followed by ethyl alcohol, and dried before use. The system was evacuated to $\sim 10^{-6}$ Torr and backfilled with an argon -10% hydrogen atmosphere. The argon had been purified by passage through titanium sponge maintained at 800°C; the hydrogen was purified with a commercial paladium diffusion unit. Melting was effected by passing a "pancake" induction coil along the length of the rod. The ingot thus produced was inverted and remelted in the opposite direction to obtain a smooth homogeneous ingot. No segregation was detectable metallographically.

Ingots were cold rolled to 0.010-in. thickness with intermediate annealing which was performed in a dynamic vacuum of $\sim 10^{-6}$ Torr. When reduction was completed, the material was sheared to strips about 2-in. long and 0.070-in. wide and subsequently recrystallized at 850°C in vacuum and furnace cooled. Specimens prepared in this manner were designated FeMo-I and FeCrMo; final compositions and grain sizes are given in Table II.

One group of FeMo-I specimens was annealed at 850°C in flowing

moist hydrogen for 24 hours and furnace cooled. These specimens were designated FeMo-II. A second group of FeMo-I specimens, together with pure iron specimens, was annealed in recirculating hydrogen in a closed quartz loop. One leg of the loop was surrounded by a resistance furnace, and contained the specimens and zirconium hydride particles. The hydrogen was repurified on each passage over these particles; it then passed over the specimens. This apparatus is similar to that described by Stein and Low[23] except that convection currents were utilized instead of mechanical pumping. This effects considerable simplification at the expense of an unknown flow rate. The treatment was carried out for 350 hours at 850°C, the specimens were then furnace cooled. The iron-molybdenum alloy exhibited a high (40,000 psi) yield strength after this treatment. Metallographic examination revealed a precipitate which was not present in the iron specimens. Microprobe analysis showed that this precipitate did not contain silicon or zirconium. Annealing the specimens in vacuum at 850°C removed the precipitate and lowered the yield strength to 23,000 psi. The specimens were used in this condition. It is believed that the precipitate was MoH_2, since hydrogen was the only other element available in significant quantities in the purification loop. The materials produced are labelled FeMo-III and Fe in Table II.

B. Apparatus and Testing Technique

A tensile machine capable of testing specimens in a vacuum of $< 10^{-5}$ Torr at temperatures up to 600°C was constructed. Rapid heating rates were attained without specimen contamination by a movable furnace within the vacuum chamber, shown in Fig. 1. The furnace was brought to the desired temperature in a position remote from the specimen and held until a vacuum of $\sim 10^{-6}$ Torr was attained. It was then lowered to surround

the specimen, bringing the latter to temperature equilibrium within 3 minutes. The pumping speed was adequate to maintain the vacuum below 10^{-5} Torr during this period, due to the small additional surface area heated. The specimen was extended the desired amount (usually 2%) at a rate of 7×10^{-4} sec^{-1}, unloaded, and then cooled by raising the furnace. The initial cooling rate (to about 200°C from a 600°C test temperature) was rapid (100°C min^{-1}) however subsequent cooling was quite slow. Possible effects of this cooling will be considered in the discussion.

Specimens were finally extended several percent at room temperature to determine the response to strain aging. Specimens intended for structural studies were only strained enough to measure the yield strength, i.e. about 1/2%.

C. Static Strain Aging Kinetics

Kinetic data were obtained on specimens strained at room temperature and then aged for various times at several temperatures. The aging response was determined by room temperature tensile tests. Similar data for the dynamic strain aging process were not obtained since the time could not be varied independently of the strain or strain rate.

Two methods of aging were used. At high temperatures, where the times of interest were too short to permit the use of the vacuum chamber in the tensile machine, specimens were strained and then encapsulated in evacuated Pyrex tubes. These were immersed in an automatically controlled salt pot, aged, and water quenched. At the two lower temperatures, the vacuum chamber was used since the heating and cooling times were no longer important relative to the total aging time. Spot checks of the longest times of each of the higher temperature runs

were made by the second method, and they gave results similar to the encapsulation method.

D. Microscopy

The structure produced by straining at selected temperatures were examined by electron transmission microscopy. Due to the small area of the specimens, the usual window and Bollman polishing techniques could not be used; it was necessary to use a modified Heidenreich technique as described by Dewey and Lewis.[24] The specimens were lightly polished mechanically to remove surface irregularities due to Luder's strain and then mounted in a Teflon holder. The holder masked the specimen except for a circular area about the size of the aperture in the microscope stage. This area was electropolished on alternate sides until a small hole was observed through a low-power telescope. Under the proper polishing conditions, the bornders of this hole contained regions thin enough for observation. An acetic acid - 10% perchloric acid electrolyte was used at 35 volts; this produced a current density of 0.1 amp/sq cm.

III. RESULTS

The principal experimental results of this investigation are the tensile properties obtained during prestrain at temperatures from 25 to 600°C and at 25°C after prestrain at all temperatures. These results are shown in Figs. 2-4, which are plots of stress vs. prestrain temperature. The two lower curves in each figure represent the stress at the indicated strains (0.2% and 2.0%) during prestrain. The top curve represents the yield strength (stress at 0.2% strain) at 25°C after prestrain. The data for FeMo-I are shown in Fig. 2, FeCrMo in Fig. 3, and Fe in Fig. 4.

The outstanding features of the alloy curves are the broad maxima in both prestrain and room temperature properties. The pure iron exhibits no such maxima. The small irregularities in the curves for iron may not be significant, since they are within the estimated error in stress measurement of ±500 psi. The alloy maxima are several times larger than this value, indicating that both alloys exhibit dynamic strain aging. To determine whether this effect was due to the intentional alloy additions or impurities, the iron molbydenum alloy was purified by annealing in hydrogen. The results of tests on the FeMo-II and III samples are shown in Figs. 5 and 6, where the coordinates and curves have the same significance as Figs. 2-4. It is seen that the 500°C maxima in prestrain and room temperature properties is still present.

The strain aging response of the various materials studied is shown in Fig. 7. The index used, $\Delta\sigma$, is the difference between the observed yield strength at 25°C after prestrain at temperature T and the flow stress observed at 2% strain at 25°C. This index measures the aging response against a zero-aging criterion, since a specimen which exhibited no aging (or recovery) would have a yield strength exactly equal to the flow stress at the completion of prestrain. The index has the disadvantage that each value of $\Delta\sigma$ involves the comparison of a specimen with a reference specimen (actually an average of several specimens) and thus any variation among specimens shows up as scatter in the aging response. However, the indices which determine the aging response with two stress measurements on the same specimen are only applicable when straining and aging do not occur simultaneously.

Referring to Fig. 7, it is seen that the strain aging response of FeMo-III is similar to that of Fe up to 300°C, but only about 16% less

than that of FeMo-I above this temperature. Purification greatly reduced the low temperature response and decreased the width of the peak at higher temperature as well as shifting the peak to slightly lower temperature (475 vs 510°C). It is also noted that the lower temperature response of the FeCrMo alloy increases approximately linearly with temperature, in contrast to the FeMo alloys; also the peak response occurs at a lower temperature (400°C vs 475 or 510°C).

In Fig. 8, the rate of strain hardening during prestrain is plotted against the prestrain temperature. The strain hardening rates increase smoothly with increasing temperature and reach maxima at temperatures corresponding to the peak strain aging response for each alloy. Pure iron exhibits an approximately constant strain hardening rate over the temperature range investigated.

All specimens exhibited some degree of Luder's strain during prestrain. The severity of this effect did not vary consistently with the straining temperature, but was generally less in FeMo-III than in the less pure FeMo specimens or in FeCrMo. The effect was smallest in the pure iron, being visible only under a hand lens (in the other alloys it was visible to the naked eye). This Luder's strain was never accompanied by serrated yielding. However, a "stair-like" curve was observed in specimens exhibiting a high degree of Luder's strain.

The alloy specimens showed a yield elongation of up to 1% upon straining at room temperature following prestrain at higher temperatures. The amount of this elongation was not reproducible in specimens prestrained at (approximately) the same temperature, and did not appear to be related to the strengthening obtained. No yield point load drops were observed under any conditions.

Measurements of the static strain aging response (prestrain at 25°C followed by aging at higher temperature) of FeMo-I were made in order to obtain the activation energy for the aging process. The response is shown in Fig. 9, where σ/σ_o, the ratio of the yield stress after straining 2% and aging at the indicated temperatures to the flow stress at 2% strain is plotted against aging time. It should be noted that initial softening (ratio < 1.0) occurred at 510 and 558°C. The time to reach 50% of the maximum value of the ratio is plotted on a logarithmic scale vs $1/T(°K^{-1})$ in Fig. 10, from which an activation energy of 42 kcal/mole is obtained, excluding the points representing the aging treatments which resulted in initial softening.

The data of Fig. 9 are plotted on a log-log scale in Fig. 11 ($\sigma/\sigma_o - 1$) is used as ordinate rather than σ/σ_o due to the log scale) in order to determine the form of the time dependence. The straight lines indicate a power law, i.e. $\sigma/\sigma_o - 1 = At^n$. At the two lower temperatures, n is about 2/3; at the higher temperatures $n \approx 1.0$.

Representative electron transmission micrographs of FeMo-III specimens prestrained at 500 and 25°C are shown in Figs. 13 and 14, respectively. The high temperature strain produced a significantly higher dislocation density. The dislocations are arranged in dense tangles rather than the more uniform distribution seen after prestrain at 25°C. The dark spots seen in Fig. 13 are believed to result from surface contamination of the foil, since no rings or streaks were observed in the diffraction pattern, as would be expected if the spots were second phase particles. Attempts to clean the foil resulted in the loss of the thin areas suitable for electron transmission.

IV. DISCUSSION

The results obtained with the pure iron will be considered first, since they form a base from which to study the alloys. Analysis of the results will then be applied to the mechanisms of static and dynamic strain aging. In connection with the latter, the question of strain enhanced diffusion will be discussed. Finally, the strengthening produced by dynamic strain aging of alloy steels will be considered in the light of the results obtained in this investigation.

A. Pure Iron

The pure iron specimens exhibit a smoothly decreasing yield and flow stress with increasing temperature, and a nearly constant room temperature yield strength after prestrain at the various temperatures. This behavior is that expected for a non-aging material and can be understood in terms of the structural studies reported by several workers. These studies have established that the dislocation density produced by a given amount of strain decreases as the temperature of the strain increases,[25,26] at the same time the minimum strain required to produce a clearly defined cell structure decreases[25] and the resulting cell diameter increases.[27] Hence, comparing iron deformed a few percent at room temperature with that deformed at 400-500°C, the former would have a higher dislocation density, with dislocations more uniformly distributed (less tendency for cell formation), while the latter would have its lower dislocation density arranged in tangles, which would become the cell walls if the strain was adequate. In terms of the room temperature strength, these factors oppose each other; that is the strength decreases as the dislocation density decreases,[25] but an additional strength is derived from

the formation of dislocation tangles or cell walls.[27] Thus at least for strains less than 10%, a relatively constant room temperature yield strength is expected. The limitation of the amount of strain arises from that fact that a cell structure is introduced at room temperature at about 10% strain,[25] and the size of these cells is less than that formed at higher temperatures.[26] The strengthening due to the presence of a cell structure is inversely proportional to the cell diameter[27] thus both factors would favor the specimen deformed at room temperature, and the yield strength after prestrain would be expected to decrease with increasing prestrain temperature.

There are two slight maxima in the room temperature yield strength (see Fig. 4) which occur at prestrain temperatures of 150 and 450°C. These maxima are not much greater than the experimental scatter, but may nevertheless be real. Interstitial impurities (~20 ppm C+N) could produce the lower maximum, while residual substitutional impurities could cause the one at higher temperature. The relation of such maxima to solutes will be considered in relation to the results obtained on the alloy specimens.

B. Iron-Molybdenum Alloys

All three iron-molybdenum alloys investigated exhibit a significant response to strain at elevated temperatures, both during this strain and in the room temperature properties after this strain, Figs. 2-7. Although no previous experiments have included the room temperature properties, the prestrain data may be compared with that reported by Glen[6,33] for a variety of ferritic alloy steels and by Baird and Jamieson[28] for iron manganese plus carbon or nitrogen. Glen reported peaks in the 400-500°C

range in all alloys investigated; he also observed peaks at lower temperatures. He ascribed the high temperature peaks to the formation of alloy carbides during strain, while the lower temperature peaks were attributed to the precipitation of iron carbides. No thin foil studies were performed to check these assignments.

Baird and Jamieson[28] observed a large 450°C peak in iron manganese nitrogen alloys, a smaller peak at 300°C in carbon containing alloys, and no peaks in iron or iron manganese alloys. No mechanisms were proposed for the high temperature peaks; however, it was pointed out that if alloy carbide or nitride precipitation were responsible, the peak temperature should be the same in both cases, since the diffusion of manganese would be the rate controlling step. In a later investigation of the iron manganese nitrogen system by electron microscopy, Baird and MacKenzie[26] observed higher dislocation densities in specimens strained at 450°C than those deformed at room temperature, but observed no precipitate either on dislocations or in the matrix in either case. They attributed the high dislocation density to interactions between the solutes and dislocation during strain.

Comparison of Glen's results on molybdenum steels with those obtained on the low carbon alloys used in the present experiments suggests that molybdenum produces a strain aging effect when present as the only solute; i.e. alloy carbide formation is not an essential part of the strengthening mechanism, although it may account for the larger effects seen by Glen than were observed in the present work. The experimental support for this hypothesis will now be considered, after which the absence of a strengthening effect in iron manganese alloys will be discussed.

The principal evidence that molybdenum is reponsible for the observed

strain aging is the fact that the aging response varied only slightly (about 16%) as the carbon level was decreased from 70 ppm to less than 10 ppm. If the aging effect were due to carbon acting either by itself or in conjunction with the molybdenum a much greater variation would have been observed. Such variation is seen in the low temperature portion of the stress vs temperature plots (i.e. 75-300°C), where the response decreased by about 65% as the carbon level was lowered from 70 to < 10 ppm.

Secondly, the activation energy obtained for the static strain aging process was 42 kcal/mole. Carbon diffusion in α iron has an activation energy of 20 kcal/mole,[29] and nitrogen about 18 kcal/mole,[30] whereas the diffusion of substitutional solutes is generally characterized by an activation energy of 57-60 kcal/mole. The difference between the observed value and the higher 57-60 kcal/mole value will be considered in the next section; at present it is sufficient to note that the temperature dependence is at least twice as great as expected for carbon diffusion, thus indicating that the diffusion of molybdenum must be rate controlling.

The fact that molybdenum diffusion is rate controlling does not rule out the possibility that carbon enters into the strengthening mechanism through the formation of molybdenum carbide. Alternatively, during dynamic strain aging the mobility of carbon atmospheres, which some evidence[31] indicates are stable up to 500°C, could be reduced by molybdenum atoms, which would be attracted to the high local carbon concentration. The latter mechanism will be considered later, where it will be shown that it is not likely to be important in the present experiments. Formation of molybdenum carbide in amounts sufficient to cause the strengthening is also improbable, at least in the high purity FeMo-III (< 10 ppm C). It must be remembered that these alloys have been furnace

cooled from 850°C. This treatment allows ample diffusion for the combination of molybdenum with most of the carbon, removing it from solution. Thus the amount of carbon available for strain aging effects should be small. This is verified by the absence of serrated yielding during strain in the 150-250°C range, and the absence of strengthening or yield point drops after strain in this temperature range, all of which are observed in iron carbon alloys.[1] It is concluded that the molybdenum is responsible for the strain aging.

The absence of a strain aging effect in Baird and Jamieson's iron manganese alloys can be explained on the basis of the different properties of the two solutes. Molybdenum has a larger atom size misfit than manganese and is a much more effective solid solution strengthener. These properties indicate that molybdenum has a much greater interaction with dislocations, and so might be expected to show strain aging directly. Manganese, due to its smaller interaction with dislocations, can only influence strain aging through an interaction with another solute, the latter (carbon or nitrogen) providing the necessary strong interaction with dislocations.

C. Iron Chromium Molybdenum Alloys

The results of tests on the FeCrMo alloy are in general similar to those for the FeMo alloys. There are, however, two significant differences. First, the low temperature (25-300°C) response increases approximately linearly with temperature rather than forming either a plateau as observed in FeMo-I or a consistently low level of aging as in FeMo-III. This behavior can be explained on the basis of chromium being a stronger carbide former and a much stronger nitride former than molybdenum. This factor plus the high concentration of chromium (5 a/o)

would be expected to lead to a more complete removal of carbon and nitrogen from solution than occurs in the iron molybdenum alloys. The aging due to these elements, which is normally observed in the low temperature region, is thus eliminated leaving the lower part of the substitutional peak clearly visible.

The second difference is the lower peak temperature in the FeCrMo alloy, (400°C vs 475-500°C in the FeMo alloys). This observation is consistent with the observed effect of chromium additions on the temperature of the secondary hardening peak in molybdenum steels.[32] It is interesting to note that Glen[33] found a maximum in the flow stress of a chromium steel at 400°C, which suggests that the chromium is producing the peak, rather than lowering the temperature of the molybdenum peak. This behavior is unexpected, since chromium has a small size misfit in the iron lattice, and so would not be expected to interact strongly with dislocations. A possible explanation is the existence of a non-equilibrium interaction between chromium and molybdenum, but no evidence for such an interaction has been observed.

D. Strengthening Mechanisms in Static Strain Aging

The time dependence of the aging response was determined from the data previously used to establish the activation energy, and is shown in Fig. 10. The ratio of the yield stress after aging to the flow stress at the completion of prestrain, minus one (due to the logarithmic plot) is plotted vs log time. It is seen that at the two lower temperatures, 350 and 375°C, a $(t)^{2/3}$ dependence is indicated. This time dependence is predicted by the Cottrell-Bilby[34] model which also predicts that the associated activation energy should be two thirds of the activation energy for diffusion of the solute causing the aging. These fractional values

arise from the fact that a solute atom moves along a path perpendicular to the equipotential lines of the hydrostatic component of the dislocation stress field. The equipotential lines are of the form

$$\eta \equiv \frac{r}{\sin \alpha} = \text{constant}$$

where r is the radial distance from the dislocation core to the solute atom, α is the angle r makes with the slip plane of the dislocation.

Solute atoms then move along paths of the form

$$\xi \equiv \frac{r}{\cos \alpha} = \text{constant}$$

By solving the diffusion problem in a coordinate system with axes n, ξ, Cottrell and Bilby showed that the number of atoms arriving at unit length of dislocation line in time t was proportional to

$$\left(\frac{ADt}{kT}\right)^{2/3}$$

where A is the interaction coefficient between a dislocation and a solute atom of volume misfit ΔV, D is the diffusivity of the solute, k is Boltzmann's constant, and T is the absolute temperature, °K.

Assuming that the strength increase due to aging is linearly related to the number of atoms arriving at dislocations, it is seen that an activation energy of two thirds the activation energy for diffusion of the solute is predicted, since

$$D^{2/3} = D_o^{2/3} e^{-2/3\left(\frac{Q}{RT}\right)} .$$

The observed activation energy, 42 kcal/mole, is very nearly equal to two thirds the activation energy for substitutional diffusion in α iron (57-60 kcal/mole). The $t^{2/3}$ time dependence is also observed, hence it can be concluded that, at least for the lower temperatures investigated, the Cottrell-Bilby mechanism is responsible for the static strain

aging. The reason why the $t^{2/3}$ time dependence is lost at the higher temperatures is not clear, but perhaps the loss can be explained on the basis of the simultaneous recovery that becomes important in this case. At still higher temperatures (500 and 550°C) this recovery is sufficient to cause initial minima in the strength vs aging time curves, and thus give a decreasing, and, ultimately, an apparent "negative" activation energy.

The conclusion drawn above (that the Cottrell-Bilby mechanism is responsible for static strain aging) only applies to the rate controlling part of the process. For example, once atoms have diffused to dislocations and formed atmospheres, these atmospheres may break up into individual clusters by diffusion along the dislocation, a process expected to be considerably more rapid than diffusion to the dislocation. The data presented gives no information on this possibility, since the atmosphere effect is expected to be large enough to account for the observed strengthening.

E. Dynamic Strain Aging

If the mechanism of dynamic strain aging were the same as that of the static case a strain enhanced diffusion effect would be demonstrated, since an equal or greater response is attained in much shorter times. However, complicating factors arise, in particular the possibility that other mechanisms contribute to the strengthening in the dynamic case. For example, Leslie and Keh[35] have reported an increased dislocation density in iron-carbon alloys strained at 200°C (where the aging due to carbon is most prominent) over that observed in the same alloy strained at room temperature and then aged at 200°C. Baird and MacKenzie[26] have reported similar findings in iron manganese nitrogen alloys strained at 450°C, again where a significant aging effect occurred. Since the strength of

metals is known to be strongly dependent on the dislocation density, it is possible that this effect accounts for the observed strengthening. Although the increased dislocation density presumably arises from an interaction between the solute(s) and dislocations during strain at elevated temperature, no model for such a process has satisfactorily related the strengthening to the diffusion of a substitutional solute element. The models which have been proposed include strain induced ordering of interstitials in a dislocation stress field, atmosphere formation on temporarily blocked (e.g. by another obstacle) dislocations, and viscous drag exerted by solute atmospheres diffusing with moving dislocations. Strain induced ordering would not apply to substitutional atoms, because of the spherical symmetry of their strain fields, unless these atoms are presumed to be associated with vacancies. A solute atom-vacancy pair would tend to reorient in a dislocation stress-field, and would thus absorb energy and provide a frictional force opposing motion of the dislocation. However, very little information on vacancies in bcc metals is available, and no solute atom-vacancy binding energies have been predicted or measured.

Atmosphere formation, on either stationary or moving dislocations, would require strain enhanced diffusion if it were to be important at the temperature of the peaks observed in this experiment (400-500°C), particularly in view of the short times of exposure (less than 1 min). The topic of strain enhanced diffusion will therefore be considered in some detail in the following paragraphs.

The diffusivity of an element in a crystal is expressed by

$$D = a_o^2 \nu C_v e^{-Em/kT} \quad (1)$$

where a_o is the lattice parameter, ν is frequency of atomic vibrations, C_v is the vacancy concentration, Em is the vacancy migration energy, and k and T have their usual significance.

Under equilibrium conditions

$$C_v = e^{-Efv/kT} \quad (2)$$

where Efv is the energy to form a vacancy.

If the vacancy concentration is increased appreciably above the equilibrium value by plastic strain, Eq. (1) shows that the diffusivity will show a similar increase. As pointed out in the introduction, the controversy centers around the question of whether the vacancy concentration can be increased sufficiently to produce measurable increases in the diffusivity.

Vacancy production can occur by several mechanisms, e.g. non-conservative motion of jogs on screw dislocations, climb of edge dislocations, annihilation of positive and negative edge dislocations superposed on adjacent slip planes, etc. It is not known which, if any, of these mechanisms is dominant, although the first one seems most probable at deformation temperatures below the creep range. The rate of vacancy production by this mechanism should be related to the strain rate and the dislocation density, which together control the frequency of intersections, some fraction of which will result in vacancy producing jogs. Some dependence on the stress level should also exist. If the stress required to continue deformation is low enough that a vacancy producing jog is a major obstacle to the motion of a dislocation, these jogs will

pin the dislocation, and few vacancies will be produced. At higher stresses, the dislocation will drag the job along with it, producing many vacancies.

The instantaneous concentration of vacancies depends on the loss rate as well as the production rate. The loss rate will be proportional to the sink density and efficiency, the excess concentration, and the temperature (through the exponential term controlling vacancy migration rates). Vacancy sinks may be dislocations, cell and grain boundaries, impurity atoms or particles, and other vacancies.

In connection with creep-diffusivity experiments, two attempts[9,10] have been made to estimate the macroscopic average vacancy concentration during strain. Unfortunately the conclusions reached in these studies are contradictory. Also, there are several factors which prevent the application of these estimates to the present experiments. The major factor is the small volumes of interest in the study of an aging reaction, e.g. of the order of 0.1 μ^3, compared to the macroscopic volumes dealt with by the estimates. Both production and loss rates would be expected to show wider variation on such a small scale. A second factor is that the non-homogeneous deformation observed in the present experiments (all specimens showed Luder's strain, to varying degrees) prevents obtaining accurate values of local strain and strain rate; which enter into the equations for the excess vacancy concentration. Finally, assumptions made in the treatments restrict their applicability to the high temperature and low strain rate region, whereas the opposite conditions are of interest here.

Enhanced diffusion may also be due to "short circuit" paths, i.e. diffusion along dislocation lines or boundaries. Rapid diffusion along

such defects has been observed in several materials.[36,37] Hart[38] has analyzed the diffusion due to this effect and obtained an expression:

$$\frac{D}{D^\circ} = 1 + f\,\frac{Dp}{D^\circ} \qquad (1)$$

where D is the observed diffusivity, D° is the normal bulk diffusivity, f is the fraction of atoms in the dislocations, and Dp is the "pipe" or dislocation diffusivity.

Under static conditions the time of diffusion must be long enough for each atom to visit several dislocations for this equation to be valid. However, if the dislocations move, they remove this condition by visiting the atoms. Since not all atoms will be visited unless very high strains are achieved, the process will be limited to some extent by volume diffusion at lower strains. In the case of a solute which is attracted to dislocations due to an elastic interaction, the pipe diffusion will be increased if the temperature is high enough for any volume diffusion to occur. Although the static case is satisfactorily covered by Eq. (1), the dynamic case requires a more extensive characterization of the deformation process; e.g. the fraction of the total number of solute atoms visited by dislocations during a given strain, the effectiveness of a dislocation in "capturing" a solute atom (which would be expected to depend on the dislocation velocity) etc., than is available.

Although boundary diffusion leads to large scale increases in macroscopic diffusivity by extending the tail of the penetration curve, it is not expected to be very important in the localized regions of interest for strengthening reactions, particularly in the present case where recrystallization does not occur during strain.

In summary, although there are several models for processes resulting

in strain enhanced diffusion, these models involve parameters which are not known or determinable in the present experiment. Depending upon the assumptions made, either large[10] or insignificant[9] enhancements of diffusion can be predicted.

However, an approximate indication of an enhanced diffusion effect can be obtained by studying the subsequent static aging response of an alloy which has been dynamically strain aged. For, if no enhanced diffusion has taken place during strain, the solute will still be distributed much as it was before strain, due to the short diffusion distances for times of ~1 minute at temperatures of 350-500°C (about ten atomic distances at the higher temperature). Thus diffusion would occur on subsequent aging, resulting in further strengthening as is observed in the static strain aging case. The absence of subsequent aging, however, would indicate that the solute has been arranged in a stable distribution during strain, which requires an enhanced diffusivity.

These experiments have been carried out at two temperatures, 350 and 375°C, and the results are shown in Fig. 12. It is seen that, within the scatter of the data, no further aging takes place in the dynamically strain aged specimens, thus indicating, as outlined above, that diffusion is enhanced during strain at these temperatures. Since the diffusion distances are expected to be somewhat smaller in the dynamically strain aged specimens, due to the higher dislocation density, it is not possible to calculate the actual enhancement from the times to complete aging in the two cases (30 seconds and 300 minutes). However, making the largest reasonable allowance for this effect, the enhancement must still be of the order of 100; i.e., the diffusivity during strain is of the order of 100 times greater than the normal diffusivity at 350°C. It should be

noted in passing that these experiments also indicate that the slow cooling in the lower temperature region of the cooling cycle which was mentioned in the procedure does not affect the results, because the specimens are, in effect, fully aged at the completion of prestrain.

The strengthening mechanism in dynamic strain aging can now be visualized as similar to that observed under static conditions, i.e. volume diffusion of molybdenum to dislocations. This process may either result in atmosphere formation, or be followed by diffusion along the dislocations to form clusters. Since the process occurs during strain, the first dislocations to be affected will act as obstacles to subsequent dislocations; thus requiring an increase in the number of fresh dislocations generated at sources in order to maintain the applied strain rate. The pinning action of molybdenum will also inhibit recovery processes at the higher strain temperatures, since these processes depend upon dislocation climb. Both effects lead to an increased dislocation density and strain hardening rate (as compared with a nonaging system). The increased dislocation density adds to the strengthening, either directly or through increasing the number of sites available for segregation of solute. These effects are believed to account for the greater strengthening observed in dynamic strain aging experiments.

It is not likely that atmospheres of substitutional solute form about moving dislocations under the present conditions, as can be shown by applying Cottrell's empirical equation[8]

$$D_{min} \simeq 10^{-9}\,\dot{\epsilon}\ \mathrm{cm}^2/\mathrm{sec}$$

where D_{min} is the minimum diffusivity for the Portevin-Le Chatelier effect, and $\dot{\epsilon}$ is the strain rate. This equation was derived from data

obtained in the iron nitrogen system. Since nitrogen diffuses interstitially, its diffusivity should not be affected by any excess vacancy concentration produced by strain. Thus, the normal diffusivity of nitrogen is used in the above equation. D_{min} for the present experiments is $\sim 10^{-12}$ cm^2/sec; the normal diffusivity of molybdenum in iron at the peak temperature observed here is $\sim 10^{-16}$ cm^2/sec. Thus an enhancement of 10^4 would be necessary for molybdenum to form an atmosphere around moving dislocations, which is considered to be the mechanism of the Portevin-Le Chatelier effect. No evidence for such enhancements exists. It thus appears that strengthening in dynamic strain aging must be associated with diffusion to dislocations which have been slowed down or stopped by some obstacles (other than by substitutional atmospheres). The same reasoning leads to the conclusion that the mechanism suggested by Baird,[1] that substitutional atoms retard the motion of dislocations which have collected mobile interstitial atmospheres, does not apply to the present experiments. If this conclusion is correct, the reduction of strengthening at temperatures above the peak must be associated with thermal vibrations overcoming the binding energy between molybdenum atoms and dislocations. At 600°C, which is just above the peak, kT is about 0.08 eV, which is of the order of the expected binding energy.

One objection to the excess vacancy model for enhanced diffusion resulting in strain aging is that an incubation strain is expected. This strain is necessary to build up the vacancy concentration up to the point where enhanced diffusion becomes significant. Such an incubation strain was not observed in the present experiment (the strengthening effect was apparent in the 0.2% yield strength at temperature) or in the experiments of Baird and Jamieson.[28] This objection may be overcome by considering small regions of the lattice where the density of moving

dislocations is high. In such regions the local strain is large and would be expected to lead to high local diffusivity and thus strain aging. No macroscopic incubation strain would then be observed. This consideration would apply particularly to cases where deformation is extremely heterogeneous (e.g. Luder's deformation) such as the present experiments. Baird and Jamieson did not state whether or not Luder's strain occurred in their alloys.

The conclusions reached in the preceding paragraphs suggest that the dynamic strain aging of alloy steels is due to the formation of alloy carbides under certain conditions of straining temperature and strain rate. Assuming that the diffusivity of alloy carbide formers in martensite is the same as in ferrite of the same composition, alloy carbide formation should become significant at straining temperatures of 300°C in molybdenum steels and at somewhat lower temperatures (~ 200°C) in chromium molybdenum steels. These temperatures apply to strain rates of $\sim 10^{-3}$ sec^{-1}. The corresponding temperatures for the much higher strain rates obtained by rolling or drawing cannot be predicted from the data obtained since the strain rate dependence of the diffusion enhancement is not known. It is suggested that quantitative measurements of the strain enhanced diffusion effect would best be made in a system where a simple single stage hardening reaction occurs (e.g. Ag-Al), in which Ag atoms form spherical clusters). Determination of the cluster size and spacing under various straining conditions should permit calculations of the diffusivity during strain. The method could be utilized at temperatures and strain rates approaching those used in the creep-diffusion experiments referred to earlier, thus providing a mutual check. Investigation of single phase (unsaturated) alloys would clearly demonstrate

the existence and approximate magnitude of the effect, since no aging would occur in such an alloy under static conditions. Clustering should occur, however, under conditions of high diffusivity at temperatures low enough for the binding (clustering) energy to be important, since a high fraction of the solute atom encounters under such conditions would lead to pair or cluster formation.

V. SUMMARY AND CONCLUSIONS

The strain aging of iron molybdenum and iron chromium molybdenum alloys has been investigated. The dynamic strain aging (straining at elevated temperatures where aging takes place simultaneously) of both alloys is similar in that a peak response is found in the 400-500°C range. This peak is of the order of 40% of the flow stress at 2% strain at room temperature. The latter value is used as a base since it represents the yield strength expected in a material which shows no aging. The experiments on pure iron verified this expectation, showing very small aging effects, of the order of the experimental scatter.

The variation of the strain aging response with interstitial content in the iron molybdenum alloys was too small to permit the response to be attributed to these solutes, either directly or indirectly. Kinetic measurements on statically strain aged specimens indicate an apparent activation energy of 42 kcal/mole, and a $(t)^{2/3}$ time dependence. These results are consistent with the Cottrell-Bilby model for strain aging, with molybdenum as the active solute. These results, taken together, indicate that molybdenum, by itself, produces strain aging in specimens strained above 300°C.

The observation that specimens strained at 350 or 375°C showed no

further aging at those temperatures (straining was completed in ~ 30 seconds) whereas completion of static aging required 250-300 minutes, is taken as evidence of strain enhanced diffusion. A lower limit of ~100 can be set for the enhancement (i.e., the diffusivity during strain is at least 100 times greater than that under static conditions at the same temperature).

It is concluded that the strengthening mechanism of dynamic strain aging involves the (enhanced) diffusion of substitutional solute to dislocations. This process occurs during strain and leads to increased dislocation densities and higher strain hardening rates in a particular temperature region. The lower limit of this region is set by diffusion considerations (enough segregation must take place during the course of the test to produce observable strengthening), while the upper limit is believed to be set by thermal vibrations overcoming the solute-dislocation binding energy.

In relation to the dynamic strain aging of steels, the results lead to the conclusion that alloy carbide formation may occur during tensile straining at temperatures (200-300°C, depending on the composition) well below the range in which such carbides are formed during static tempering (450-500°C, for one hour tempering). Such carbide formation is believed to account for an appreciable part of the strengthening observed in dynamic strain aging.

ACKNOWLEDGEMENTS

The author is indebted to Professor E. R. Parker and Dr. V. F. Zackay for helpful discussions throughout the course of this study. He also would like to thank the Bureau of Mines for supplying the high purity chromium used, Mr. Y. Chung for assistance in phases of the experimental work, and Mrs. Gloria Pelatowski for preparing the figures.

This work was performed under the auspices of the United States Atomic Energy Commission.

BIBLIOGRAPHY

1. J. D. Baird, Iron and Steel, 36, 186, 326, 450 (1963).

2. E. T. Stephenson and M. Cohen, Trans. ASM, 54, 72 (1961).

3. V. Goel, R. Busch and V. F. Zackay (to be published in Trans. ASME).

4. J. L. Peterson, Trans. ASM, 56, 304 (1963).

5. L. J. Dijkstra and R. J. Sladek, Trans. AIME, 197, 69 (1953).

6. J. Glen, ASTM Spec. Tech. Pub. No. 128, 1952, Pg. 184.

7. G. Ardley and A. H. Cottrell, Proc. Roy. Soc. A219, 328 (1953).

8. A. H. Cottrell, Phil. Mag. 44, 829 (1953).

9. R. W. Baluffi and A. L. Ruoff, J. App. Phys., 34, 1634, 1848, 2862 (1963).

10. Y. P. Romashkin, Fiz Tverdogo Tela, 2, 3050 (1961).

11. K. Hirano, M. Cohen, B. L. Averbach and N. Ujiiye, Trans. AIME, 227, 950 (1963).

12. C. H. Lee and R. Maddin, Trans. AIME, 215, 396 (1959); Also J. App. Phys. 32, 1846 (1960).

13. A. F. Forestieri and L. A. Girifalco, J. Phys. Chem. Sol. 10, 99 (1959).

14. A. R. Wazzan, J. Mote and J. E. Dorn, ASTIA 257188, April 18, 1961.

15. J. B. Darby, C. T. Tomizuka and R. W. Balluffi, J. App. Phys. 32, 840 (1961).

16. P. Chollet, I. Grosse and J. Philibert, Compt. Rend. 252, 728 (1961).

17. S. Pearson, A. J. Board and C. Wheeler, Phil. Mag. 6, 979 (1961).

18. A. V. Savitskii, Fiz. Metal. i Metalloved, 10, 564 (1960).

19. V. B. Nileshwar and A. G. Quarrel, ISI Spec. Rep. 64, 259 (1959).

20. E. E. Underwood and G. K. Manning, Bettelle Mem. Inst. Rep. NACA Project NAW6515, August 1958.

21. R. W. Honeycombe, H. J. Harding and J. J. Irani in High Strength Materials, V. F. Zackay, Ed. (John Wiley and Sons, New York, 1965), p. 213.

22. A. Berghezan and E. B. Simonsen, Trans. AIME, 221, 1029 (1961).

23. D. F. Stein, J. R. Low and A. U. Seybolt, Acta Met. 11, 1253 (1963).

24. M. A. Dewey and T. G. Lewis, J. Sci. Inst. 40, 385 (1963).

25. A. S. Keh and S. Weissman in Electron Microscopy and Strength of Crystals, G. Thomas and J. Washburn, Ed. (Interscience Publishers, New York, 1963) p. 231.

26. J. O. Baird and C. R. MacKenzie, JISI 202, 427 (1964).

27. D. H. Warrington, JISI, 201, 610 (1963).

28. J. D. Baird and A. Jamieson in The Relation Between the Structure and Mechanical Properties of Metals, NPL Symposium, January 1963(HMSO).

29. C. A. West, Phys. Rev. 76, 1169 (1949).

30. J. O. Fast and M. B. Verrijp, JISI 176, 24 (1954).

31. M. J. Manjoine, Trans. ASME, 66, 241A (1944).

32. E. C. Bain and H. W. Paxton in Alloying Elements in Steel (ASM 1961) p. 200.

33. J. Glen, JISI 186, 21 (1957).

34. A. H. Cottrell and B. A. Bilby, Proc. Phys. Soc. A62, 49 (1949).

36. R. L. Segall, P. G. Partridge and P. B. Hirsch, Phil. Mag. 6, 1493 (1961).

37. O. Turnbull and R. E. Hoffman, Acta Met. 2, 419 (1954).

38. E. W. Hart, Acta Met. 5, 597 (1957).

Table I. Processing and analyses of materials used for alloy preparation

		C	N	O	H	ppm
Fe	electron beam zone refined	5	< 1	6	-	
Cr	electrolytic	-	-	150	-	
Mo	electron beam melted	< 10	< 10	< 5	-	

Table II. Composition, final heat treatment, and average grain diameter for the materials investigated

		All treatments at 850°C	ppm (wt) C	N	O	H	Grain diam. μ
FeMo-I		Recrystallized in vacuum	70	16	38	5	28
FeMo-II	2.2 a/o Mo	Wet hydrogen 24 hrs	20	45	-	-	39
FeMo-III		Dry hydrogen 350 hrs and 6 hrs vacuum	< 10	< 20	-	-	43
FeCrMo	4.9 a/o Cr, 1.3 a/o Mo	Recrystallized in vacuum	50	25	< 20	-	31
Fe		Dry hydrogen 350 hrs	< 10	< 10	-	-	64

FIGURE CAPTIONS

Fig. 1 Vacuum tensile machine, showing the movable furnace feature.

Fig. 2 Tensile properties of FeMo-I (2 a/o Mo 70 ppm C, 15 ppm N). The bottom curve represents the yield strength (0.2% strain) at the prestrain temperature; the middle curve represents the stress at 2% strain, also at temperature. The top curve represents the yield strength at 25°C after prestraining 2% at the indicated temperatures.

Fig. 3 Tensile properties of FeCrMo (4.9 a/o Cr, 1.3 a/o Mo, 50 ppm C, 25 ppm N). Curves have same significance as in Fig. 1.

Fig. 4 Tensile properties of Fe (< 10 ppm C, < 10 ppm N). Curves have same significance as in Fig. 1.

Fig. 5 Tensile properties of FeMo-II (2 a/o Mo, 20 ppm C, 45 ppm N). The curves have the same significance as previous figures.

Fig. 6 Tensile properties of FeMo-III (2 a/o Mo < 10 ppm C, < 20 ppm N). Curves have same significance as in previous figures.

Fig. 7 Strain aging response of alloys strained 2% at the indicated temperatures. The response, $\Delta\sigma$, is the yield strength at 25°C after prestrain minus the 2% flow stress at 25°C. See text for discussion of this index.

a) Fe, FeMo-I, and FeMo-III; b) Fe and FeCrMo

See Table II for compositions

Fig. 8 Rate of strain hardening of pure iron and the alloys during prestrain. The peak values for the alloys occur at temperatures similar to the respective peaks in strain aging response.

a) Fe, FeMo-I and FeMo-III; b) Fe and FeCrMo

See Table II for compositions

Fig. 9 Aging response of FeMo-I after 2% strain at 25°C (static strain aging). σ/σ_o, the ratio of the yield strength after aging to the 2% flow stress during prestrain is plotted versus aging time at several temperatures.

Fig. 10 Arrhenius plot of the data in Fig. 7. $t_{50\%}$ refers to the time required to attain one half of the maximum aging response. See text for discussion of the data at 558 and 507°C.

Fig. 11 The data of Fig. 7 plotted on a log-log scale to determine the time dependence. The data indicate a $t^{2/3}$ dependence at the lower two temperatures.

Fig. 12 A comparison of the aging response of FeMo-I at 350 and 375°C. a) Strained at room temperature and then aged, b) Strained at the aging temperature and then aged. The completion of prestrain is taken as zero time.

Fig. 13 Transmission micrograph of a FeMo-III specimen strained 2% at 498°C. A high dislocation density and well developed tangles are observed.

Fig. 14 Transmission micrograph of a FeMo-III specimen strained 2% at 25°C. The dislocation density and distribution is similar to that observed in pure iron.[25]

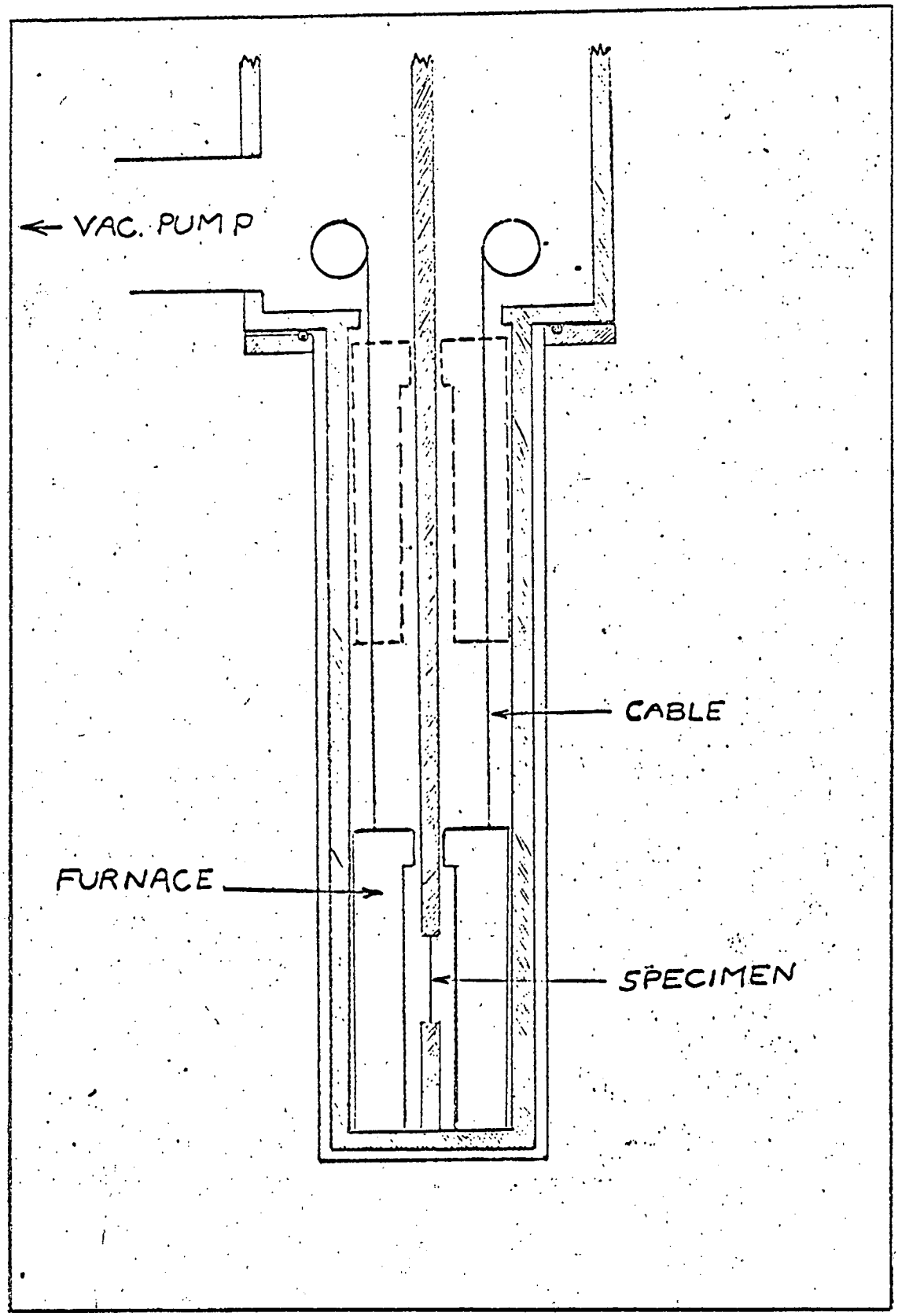

Fig. 1

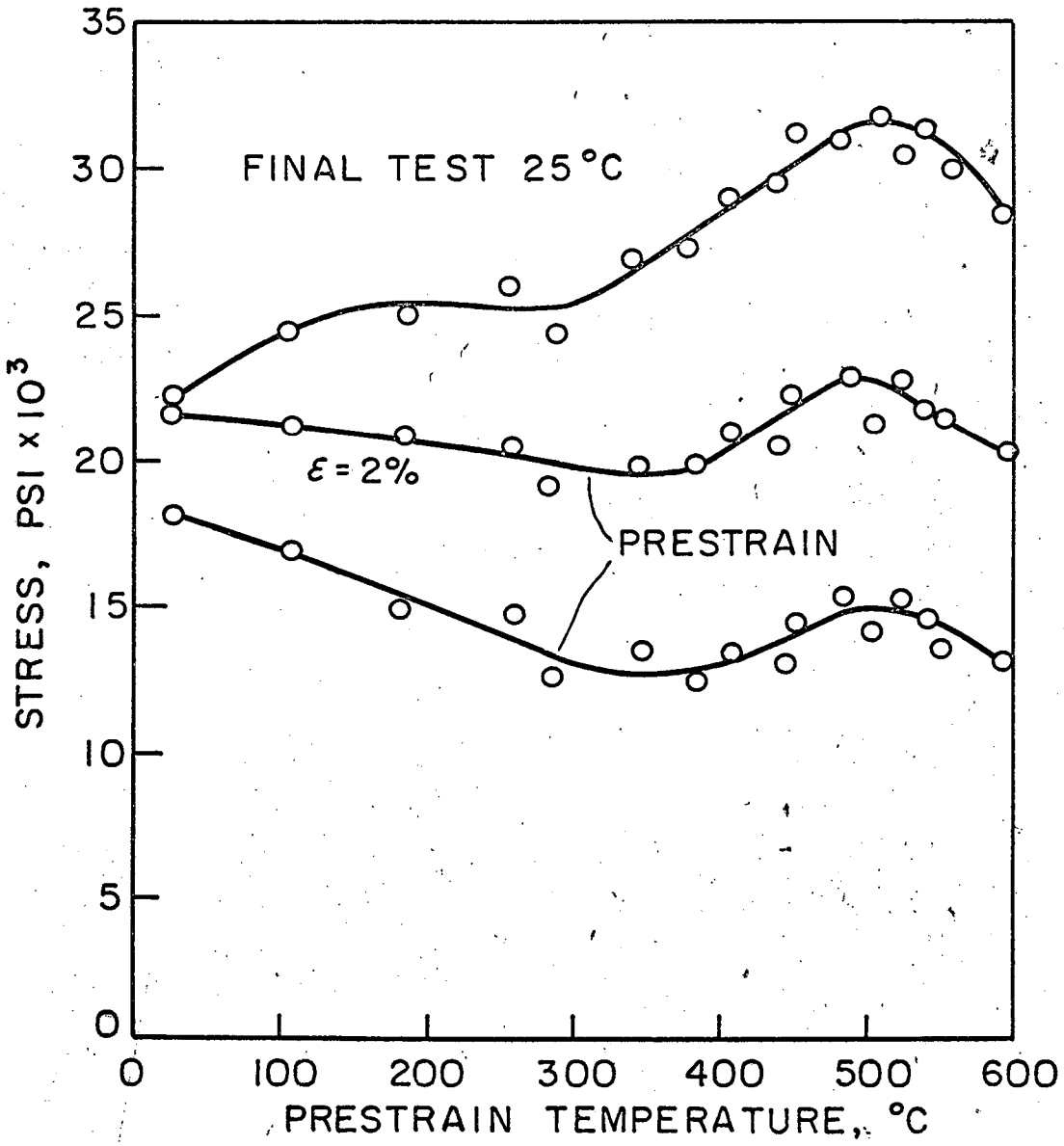
FINAL TEST 25°C
ε = 2%
PRESTRAIN
STRESS, PSI x 10³
PRESTRAIN TEMPERATURE, °C
0
5
10
15
20
25
30
35
0
100
200
300
400
500
600

Fig. 2

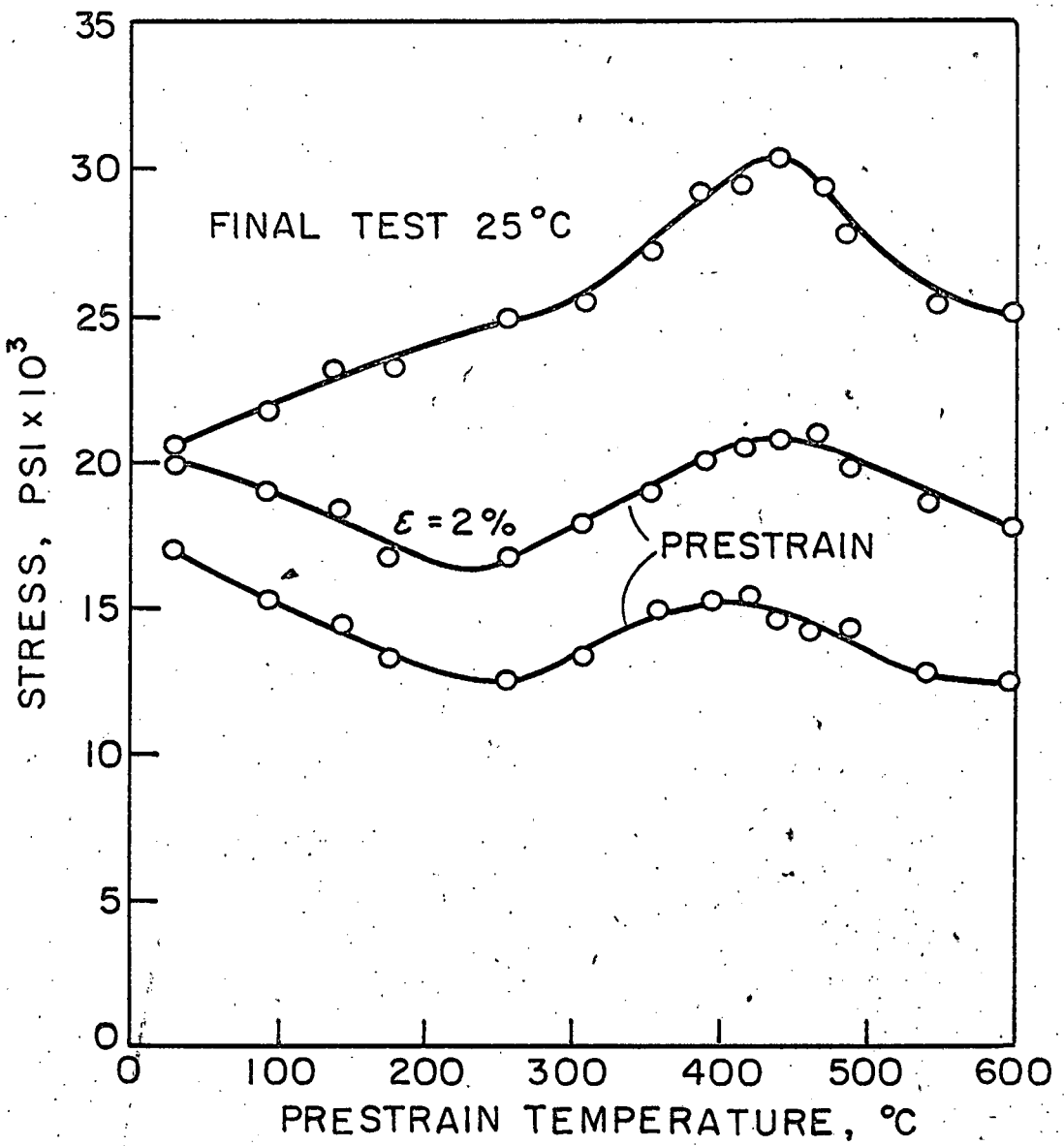
35
30
25
20
15
10
5
0
STRESS, PSI x 10^3
FINAL TEST 25°C
ε = 2%
PRESTRAIN
0
100
200
300
400
500
600
PRESTRAIN TEMPERATURE, °C

Fig. 3

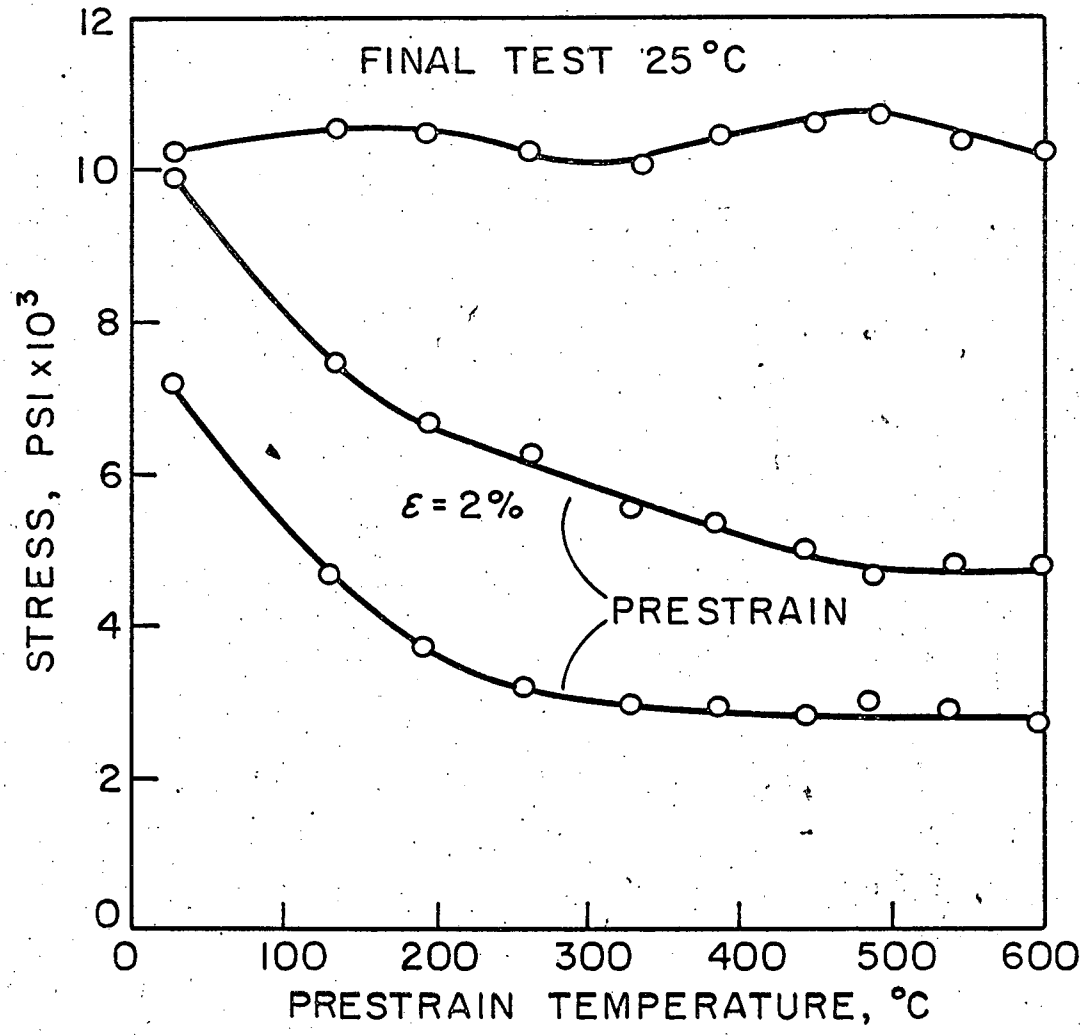
FINAL TEST 25 °C
ε = 2%
PRESTRAIN
STRESS, PSI x 10³
PRESTRAIN TEMPERATURE, °C
0
2
4
6
8
10
12
0
100
200
300
400
500
600

Fig. 4

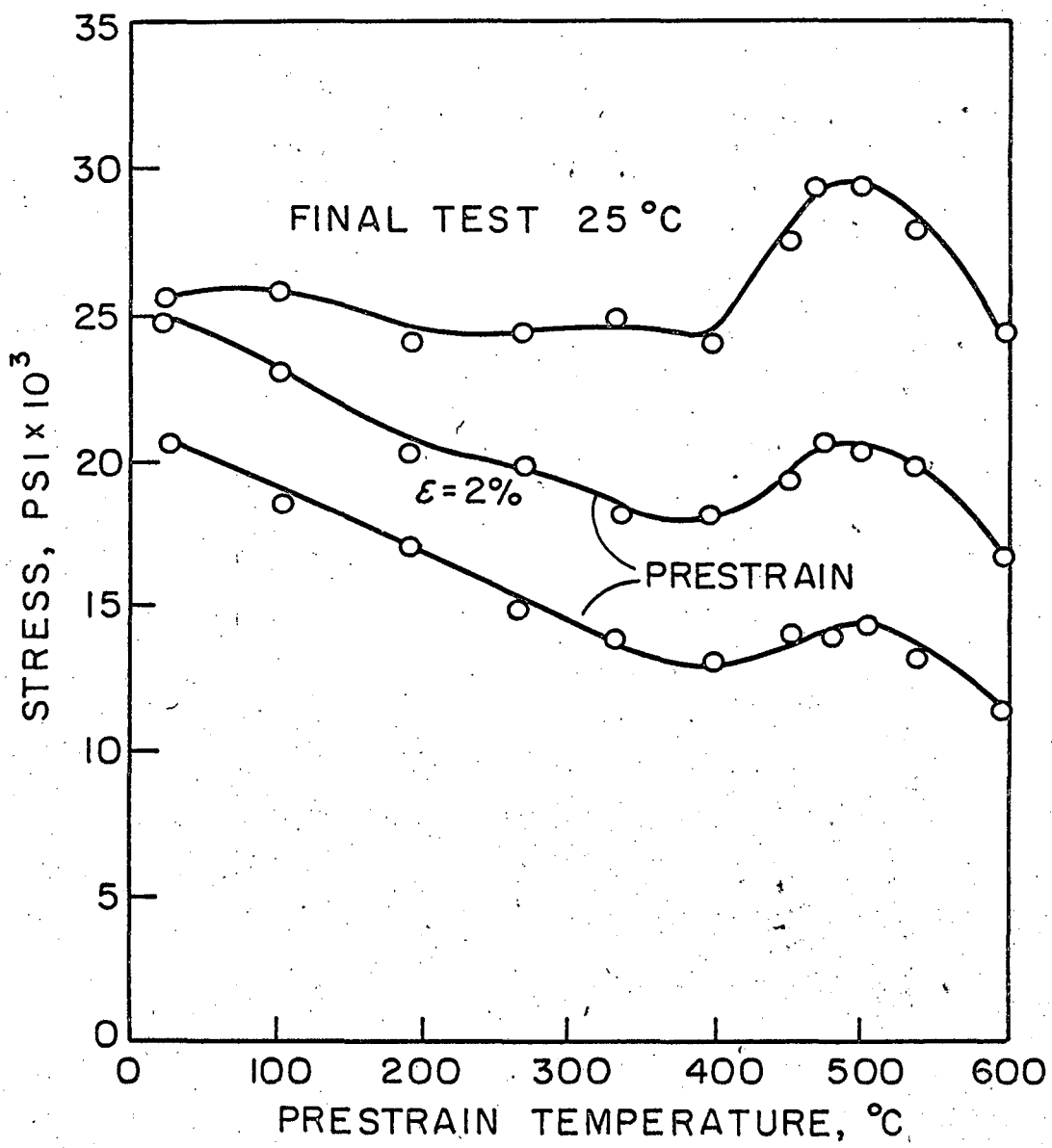
FINAL TEST 25 °C
ε = 2%
PRESTRAIN
STRESS, PSI x 10^3
PRESTRAIN TEMPERATURE, °C
0
5
10
15
20
25
30
35
0
100
200
300
400
500
600

Fig. 5

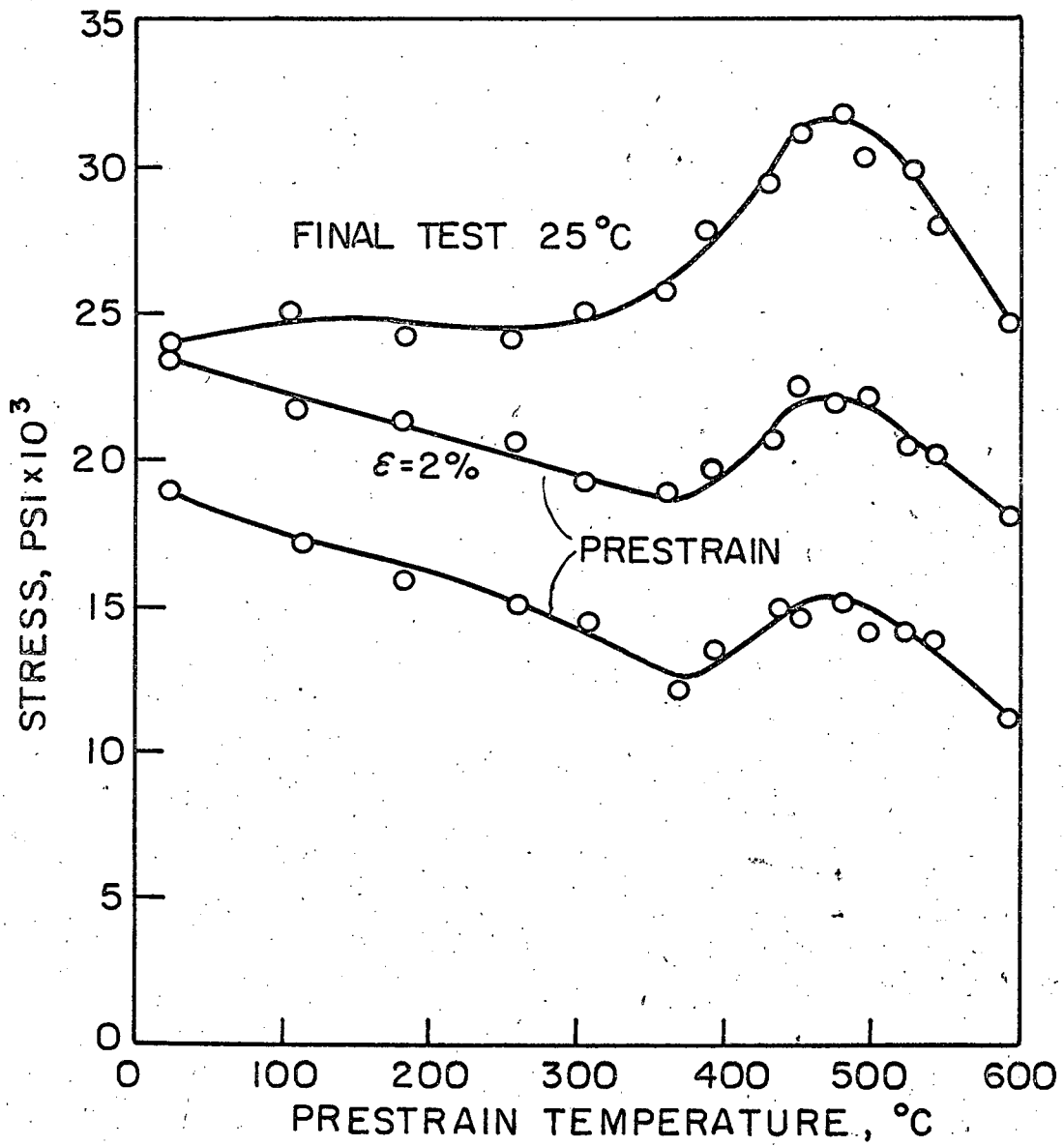
35
30
25
20
15
10
5
0
STRESS, PSI x 10^3
FINAL TEST 25°C
ε=2%
PRESTRAIN
0
100
200
300
400
500
600
PRESTRAIN TEMPERATURE, °C

Fig. 6

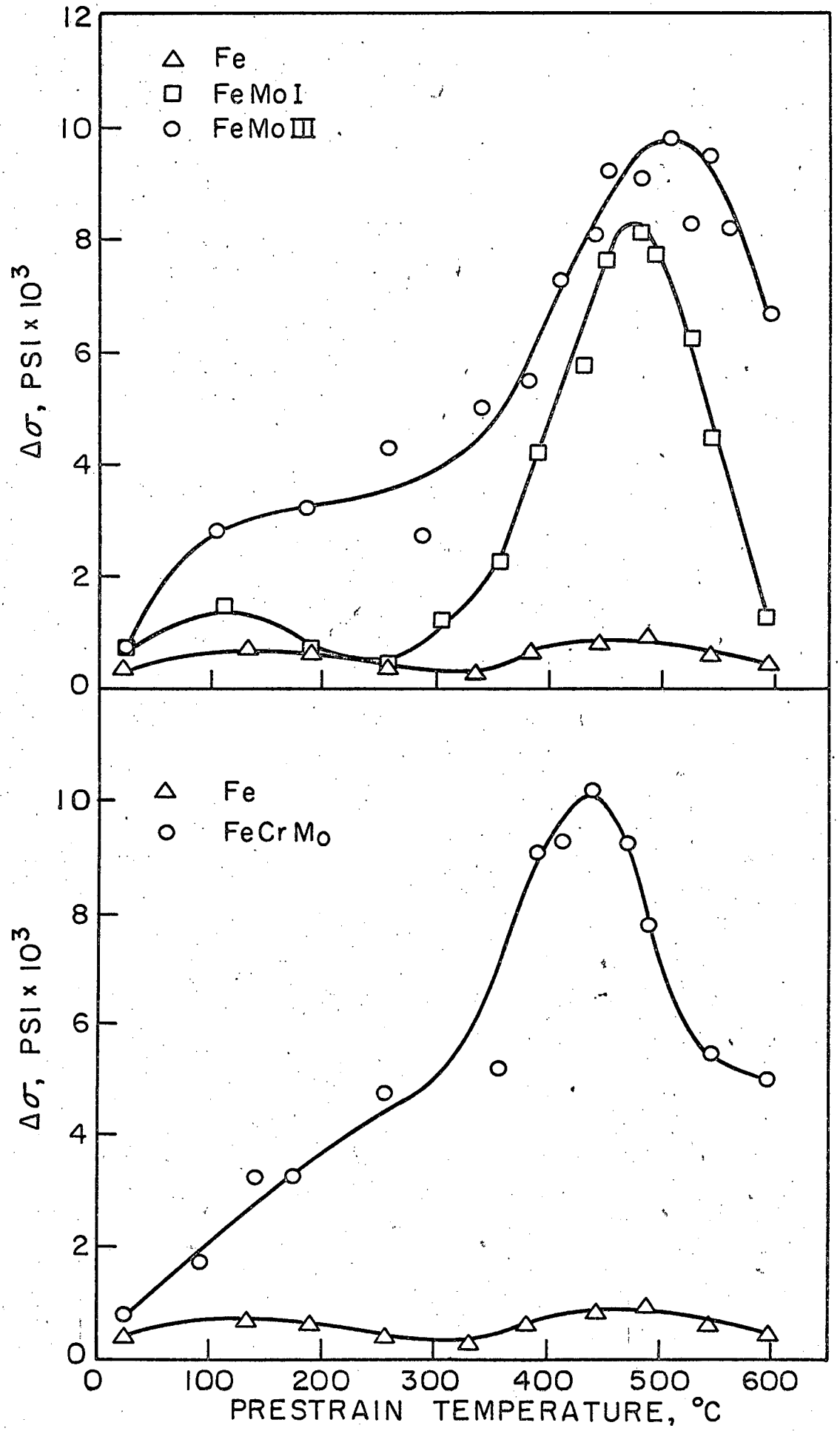
Fe
FeMoI
FeMoIII
Fe
FeCrMo
Δσ, PSI x 10^3
PRESTRAIN TEMPERATURE, °C
0
2
4
6
8
10
12
100
200
300
400
500
600

Fig. 7

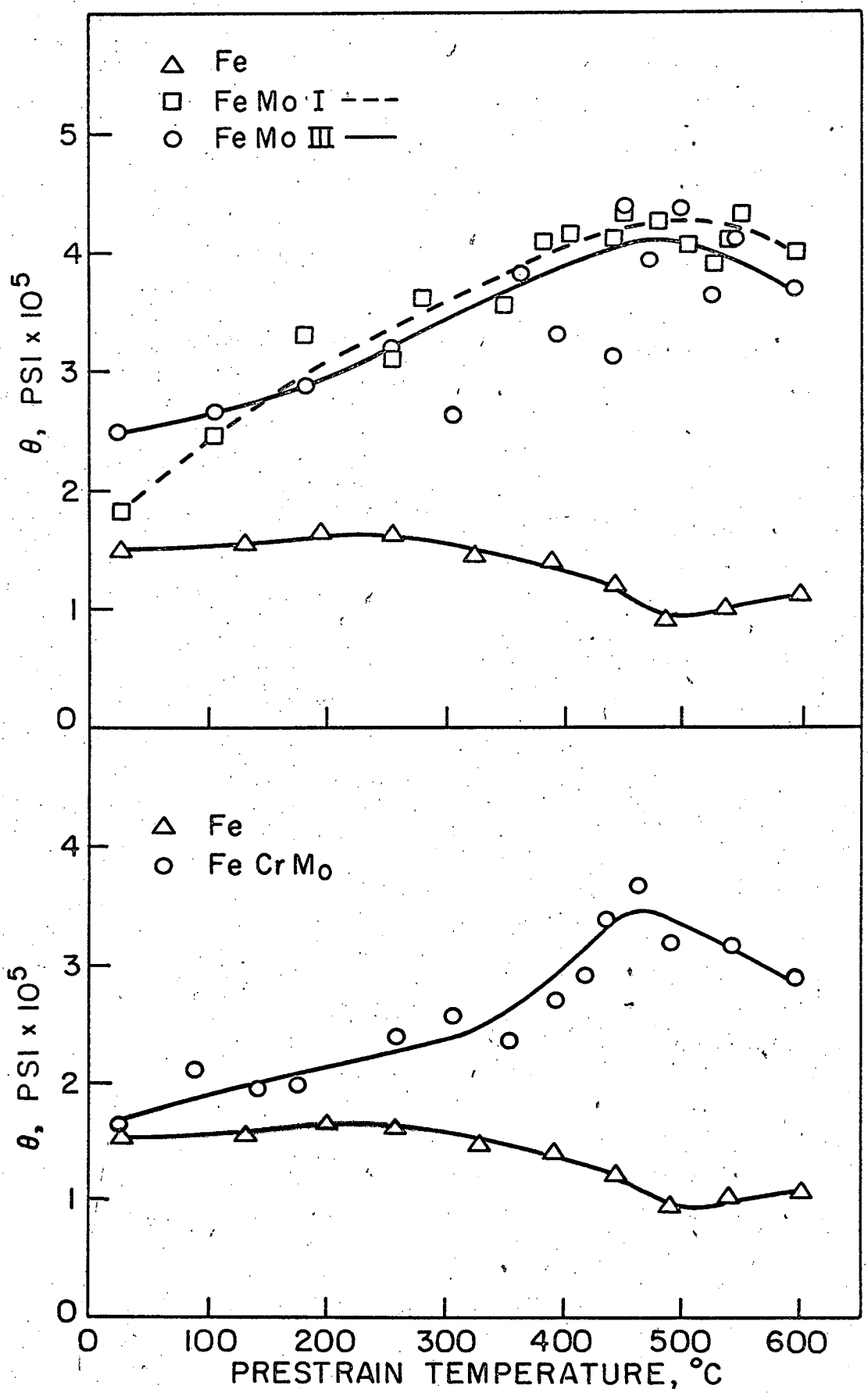
Fe
Fe Mo I
Fe Mo III
θ, PSI x 10^5
0
1
2
3
4
5
Fe
Fe Cr Mo
θ, PSI x 10^5
0
1
2
3
4
0
100
200
300
400
500
600
PRESTRAIN TEMPERATURE, °C

Fig. 8

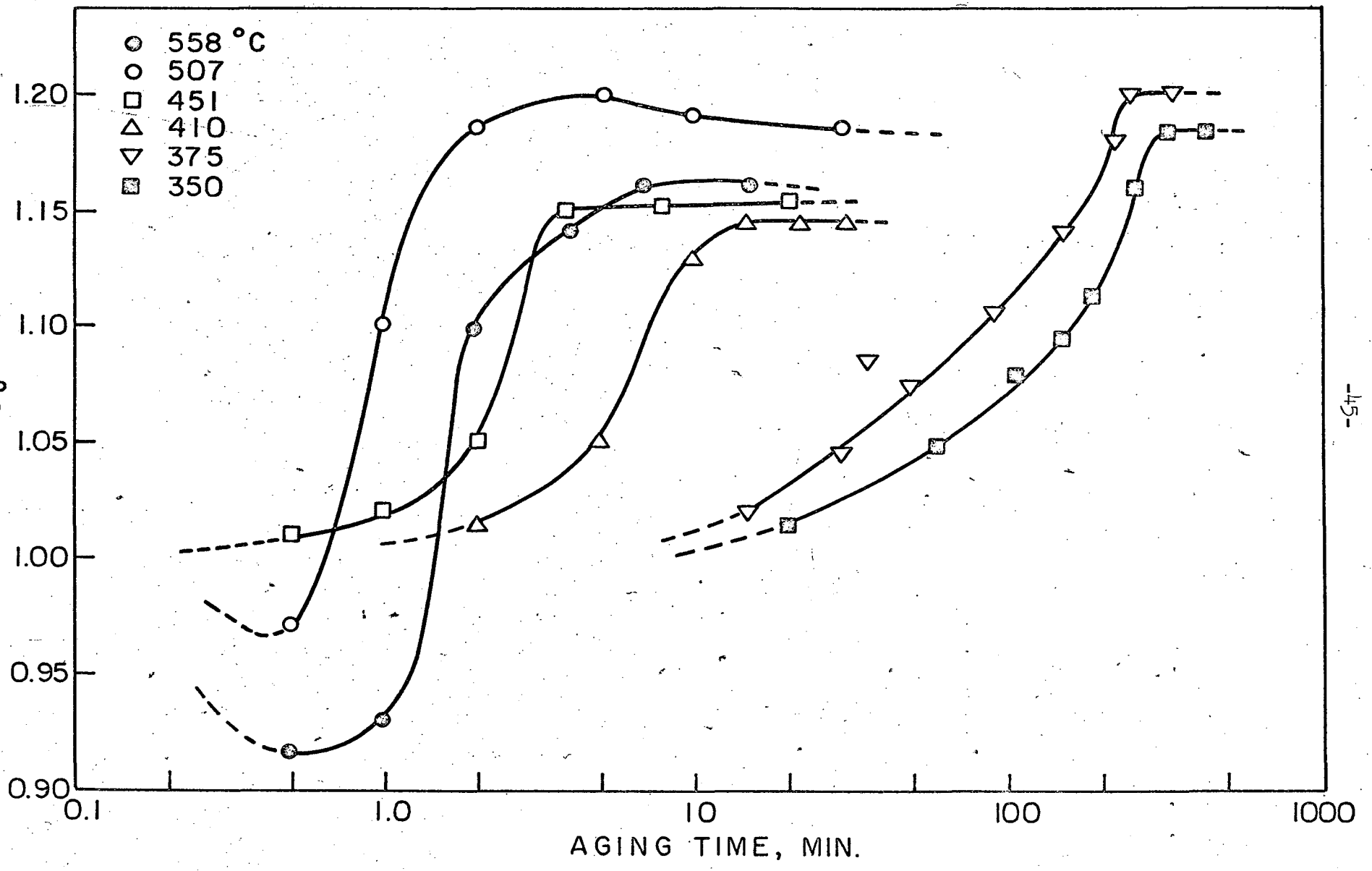
558 °C
507
451
410
375
350
1.20
1.15
1.10
1.05
1.00
0.95
0.90
σ/σ°
0.1
1.0
10
100
1000
AGING TIME, MIN.

Fig. 9

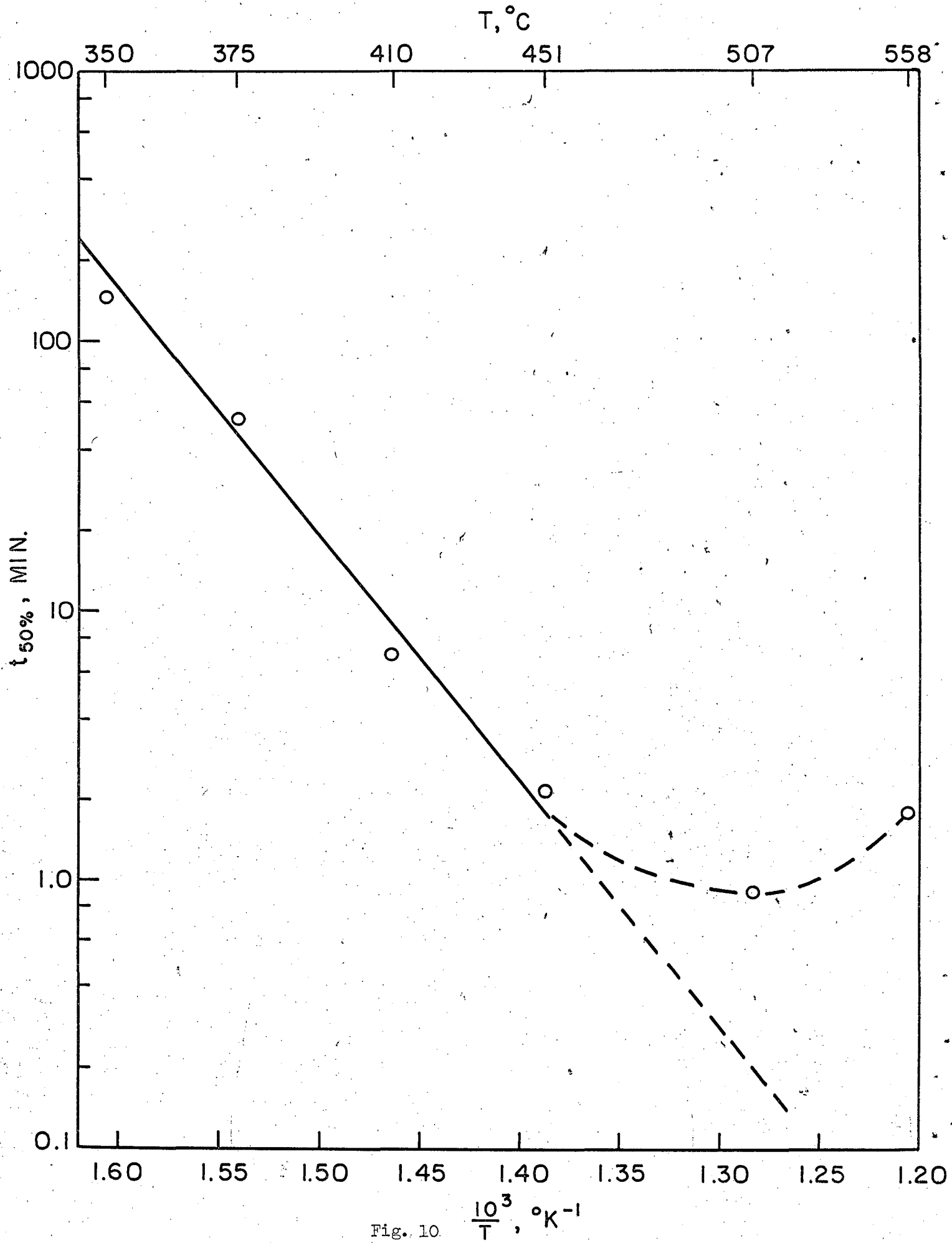
T, °C
350
375
410
451
507
558
1000
100
10
1.0
0.1
$t_{50\%}$, MIN.
1.60
1.55
1.50
1.45
1.40
1.35
1.30
1.25
1.20
$\frac{10^3}{T}$, °K^{-1}

Fig. 10

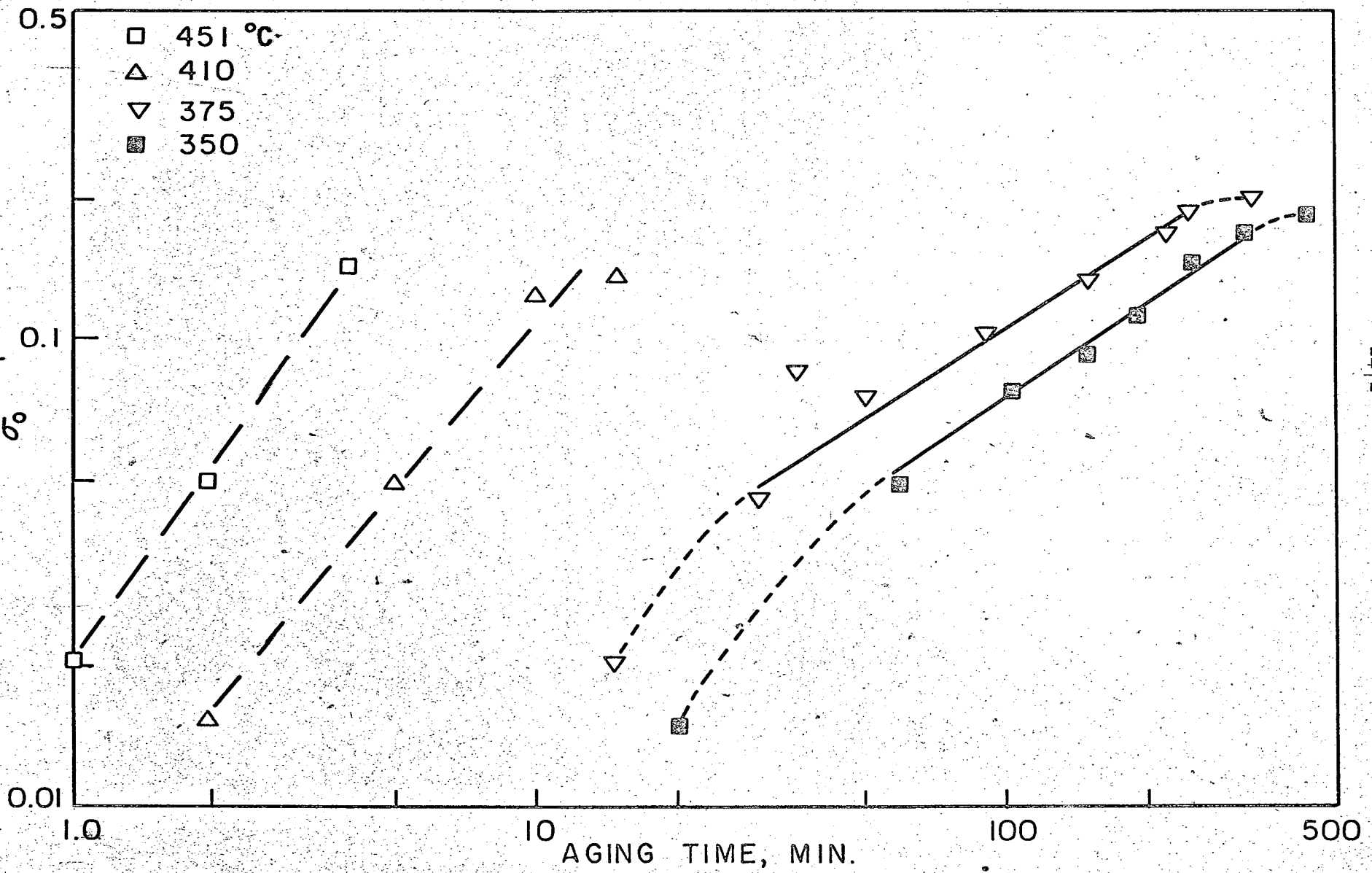
451 °C
410
375
350
0.5
0.1
0.01
σ/σ_0
1.0
10
100
500
AGING TIME, MIN.

Fig. 11

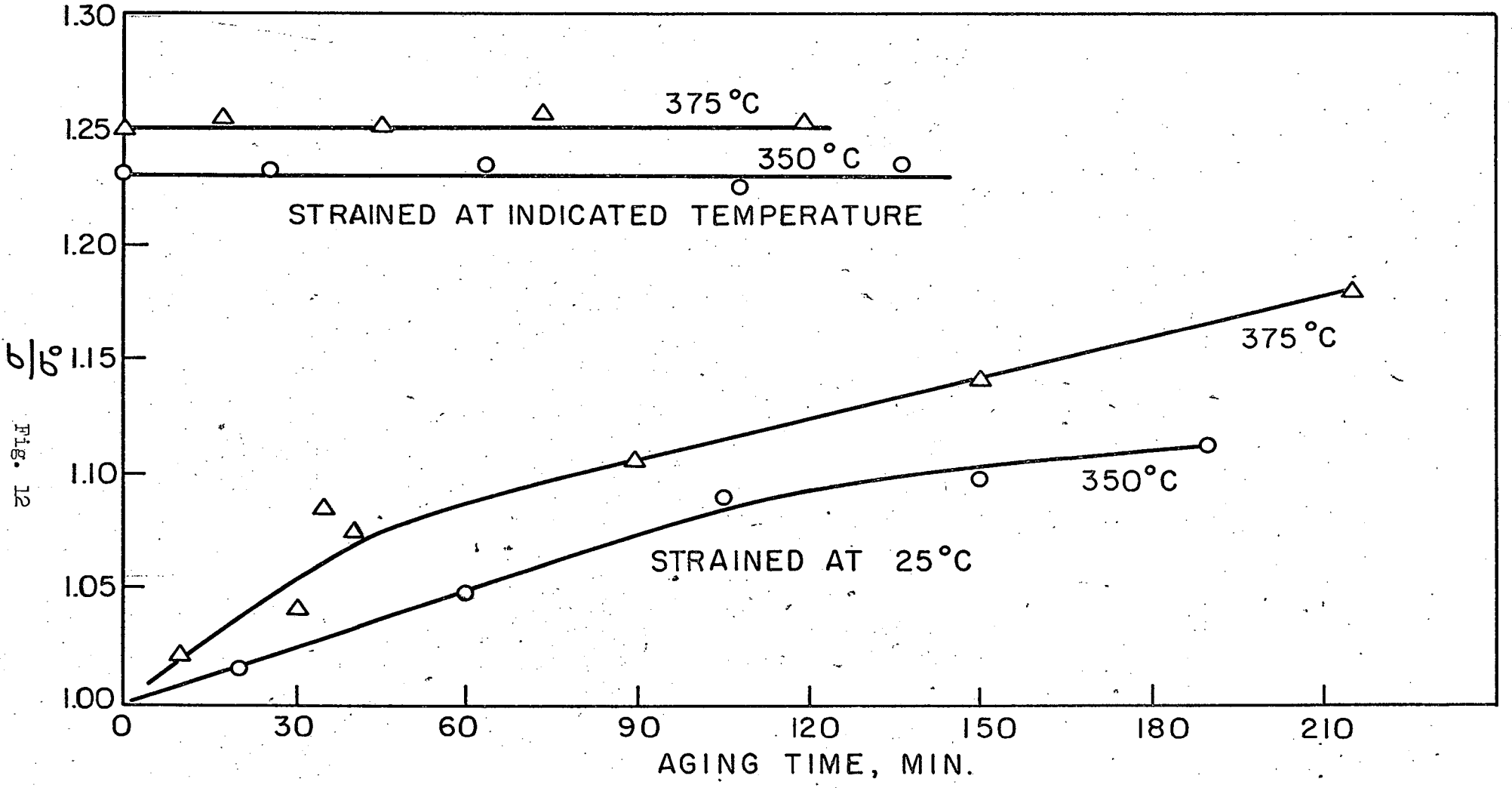
1.30
1.25
1.20
1.15
1.10
1.05
1.00
σ/σ°
375 °C
350 °C
STRAINED AT INDICATED TEMPERATURE
375 °C
350°C
STRAINED AT 25°C
0
30
60
90
120
150
180
210
AGING TIME, MIN.

Fig. 12

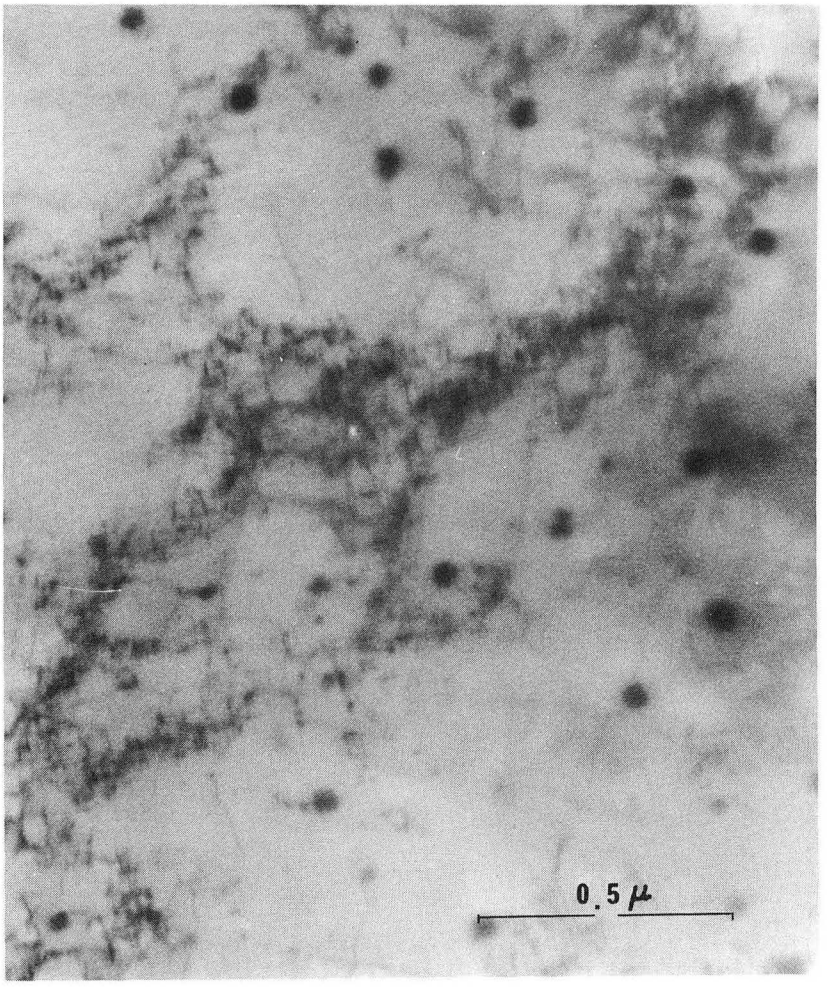

ZN-5366

Fig. 13

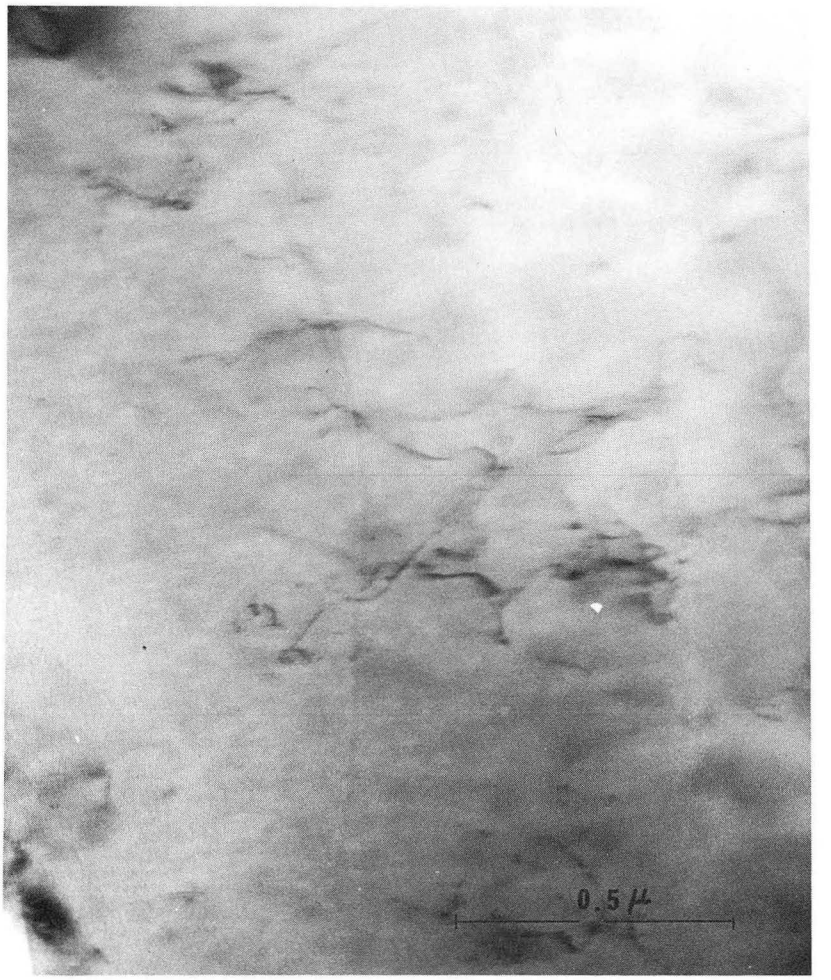

ZN-5367

Fig. 14

This report was prepared as an account of Government sponsored work. Neither the United States, nor the Commission, nor any person acting on behalf of the Commission:

A. Makes any warranty or representation, expressed or implied, with respect to the accuracy, completeness, or usefulness of the information contained in this report, or that the use of any information, apparatus, method, or process disclosed in this report may not infringe privately owned rights; or

B. Assumes any liabilities with respect to the use of, or for damages resulting from the use of any information, apparatus, method, or process disclosed in this report.

As used in the above, "person acting on behalf of the Commission" includes any employee or contractor of the Commission, or employee of such contractor, to the extent that such employee or contractor of the Commission, or employee of such contractor prepares, disseminates, or provides access to, any information pursuant to his employment or contract with the Commission, or his employment with such contractor.